Spectrochimica Acta Part A: Molecular and Biomolecular Spectroscopy 258 (2021) 119831

Contents lists available at ScienceDirect

Spectrochimica Acta Part A: Molecular and Biomolecular Spectroscopy

journal homepage: www.elsevier.com/locate/saa

Surface-enhanced Raman spectroscopy for the identification of tigecycline-resistant *E. coli* strains

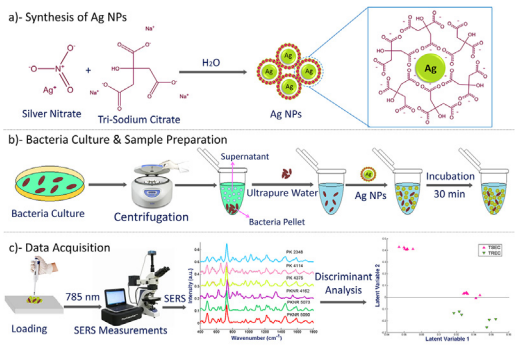
Saba Bashir [a], Haq Nawaz [a,*], Muhammad Irfan Majeed [a,*], Mashkoor Mohsin [b,*], Ali Nawaz [b], Nosheen Rashid [c], Fatima Batool [a], Saba Akbar [a], Muhammad Abubakar [a], Shamsheer Ahmad [a], Saqib Ali [a], Muhammad Kashif [a]

[a] Department of Chemistry, University of Agriculture Faisalabad, Faisalabad 38040, Pakistan
[b] Institute of Microbiology, University of Agriculture Faisalabad, Faisalabad 38040, Pakistan
[c] Department of Chemistry, University of Central Punjab, Faisalabad Campus, Faisalabad, Pakistan

HIGHLIGHTS

- Different TREC and TSEC strains have been differentiated by employing SERS.
- Silver nanoparticles (Ag NPs) are used as SERS substrate to enhance the Raman signal.
- Spectra of all strains are compared to determine features related to TGC resistance.
- The qualitative discrimination among all the strains is done by both PCA and HCA.
- PLS-DA successfully discriminated the TREC and TSEC strains with 100% accuracy.

GRAPHICAL ABSTRACT



ARTICLE INFO

Article history:
Received 15 February 2021
Received in revised form 9 April 2021
Accepted 10 April 2021
Available online 24 April 2021

Keywords:
Surface Enhanced Raman Spectroscopy
Discriminant analysis
Escherichia coli
Tigecycline resistance

ABSTRACT

Tigecycline (TGC) is recognised as last resort of drugs against several antibiotic-resistant bacteria. Bacterial resistance to tigecycline due to presence of plasmid-mediated mobile TGC resistance genes (*tet X3/X4*) has broken another defense line. Therefore, rapid and reproducible detection of tigecycline-resistant *E. coli* (TREC) is required. The current study is designed for the identification and differentiation of TREC from tigecycline-sensitive *E. coli* (TSEC) by employing SERS by using Ag NPs as a SERS substrate. The SERS spectral fingerprints of *E. coli* strains associated directly or indirectly with the development of resistance against tigecycline have been distinguished by comparing SERS spectral data of TSEC strains with each TREC strain. Moreover, the statistical analysis including Principal Component Analysis (PCA), Hierarchical Cluster Analysis (HCA) and Partial Least Squares-Discriminant Analysis (PLS-DA) were employed to check the diagnostic potential of SERS for the differentiation among TREC and TSEC strains. The qualitative identification and differentiation between resistant and sensitive strains and among individual strains have been efficiently done by performing both PCA and HCA. The successful discrimination among TREC and TSEC at the strain level is performed by PLS-DA with 98% area under ROC curve, 100% sensitivity, 98.7% specificity and 100% accuracy.

© 2021 Elsevier B.V. All rights reserved.

* Corresponding authors.
E-mail addresses: irfan.majeed@uaf.edu.pk (M. Irfan Majeed), mashkoormohsin@uaf.edu.pk (M. Mohsin).

https://doi.org/10.1016/j.saa.2021.119831
1386-1425/© 2021 Elsevier B.V. All rights reserved.

1. Introduction

Tigecycline (TGC), the first member of glycylcyclines, is a broad-spectrum semisynthetic antibiotic that has strong in vitro antimicrobial activity against an expanded spectrum of pathogens including anaerobic, aerobic, gram-negative, gram-positive and atypical bacteria [1]. It can inhibit amino acid synthesis by obstructing tRNA's entry into the A site of ribosome through its reversible binding to 30S bacterial ribosomal subunit, similar to tetracyclines [2]. The US Food and Drug Administration (FDA) has approved TGC, a 9-t-butylglycylamido derivative of minocycline, for the treatment of community-associated bacterial pneumonia, complex intra-abdominal, soft tissue and skin infections in 2005 [3–5]. TGC has been regarded as a last resort drug against difficult-to-treat infections caused by carbapenemase (especially NDM) producing and extended-spectrum beta-lactamase (ESBL) producing *E. coli* which have been emerged recently and have limited treatment options [6]. It is also active against vancomycin-resistant *enterococci*, penicillin-resistant *Streptococcus pneumonia* and methicillin-resistant *Staphylococcus aureus* [7]. The effectiveness of antibiotics is undermining due to the dissemination and emergence of antibiotic resistance genes. In multi-drug resistant (MDR) Enterobacteriaceae, another defense line has been broken due to the presence of *tet(X3)* and *tet(X4)* which are plasmid-mediated mobile TGC resistance genes [8,9]. Initially, obligate anaerobic *Bacteroides* were found to have *tet(X)* in 1984 [10] and till 2007 their existence was not reported in aerobic strains [11]. Now, different strains of Enterobacteriaceae, Flavobacteriaceae, Comamonadaceae and Moraxellaceae have seven variants of *tet(X)* genes including *tet(X1)*, *tet(X2)*, *tet(X3)*, *tet(X4)*, *tet(X5)*, *tet(X6)* and *tet(X7)* [8,9,12–16].Fig. 1.Table 1.

Table 1
Details of *E. coli* strains used for the comparison.

Strain No.	Strain ID	Specie	TREC/TSEC
1	PKNR 5090	*E. coli*	TSEC
2	PKNR 5073	*E. coli*	TSEC
3	PKNR 4162	*E. coli*	TSEC
4	PK 4375	*E. coli*	TREC
5	PK 4114	*E. coli*	TREC
6	PK 2248	*E. coli*	TREC

Pathogens confer TGC resistance through various mechanisms that involve mutations in plasmid-mediated resistance genes such as *tet(X)*, plsC, trm and rpsJ that encoding flavin-dependent monooxygenase (FMO), 1-acyl-*sn*-glycerol-3-phosphate acyltransferase, SAM-dependent methyltransferase and ribosomal S10 protein which are causing TGC resistance in *E. coli* [17–21]. Additionally, overexpression of efflux pumps e.g., multidrug and toxin extrusion (MATE) pumps, AcrAB-TolC and resistance-nodulation-cell division (RND) pumps in bacteria can also cause TGC resistance [3,22,23].

Although conventional bacterial identification culture-based molecular assays including mass spectroscopy, enzyme-linked immunosorbent assay (ELISA) and polymerase chain reaction (PCR) are used as a standard for antibiotics susceptibility testing, they lack specificity and require long incubation time that delays the confirmation of results [24–27]. Over the past years, several nanocrystal-based assays have been used for the detection of bacteria due to chemical stability and intrinsic rich optical properties of nanocrystals [28] including colorimetric, fluorescence [29], photoluminescence, light-scattering [30] and vibrational spectroscopy [31–33]. The high rate of false positives due to increased luminesce

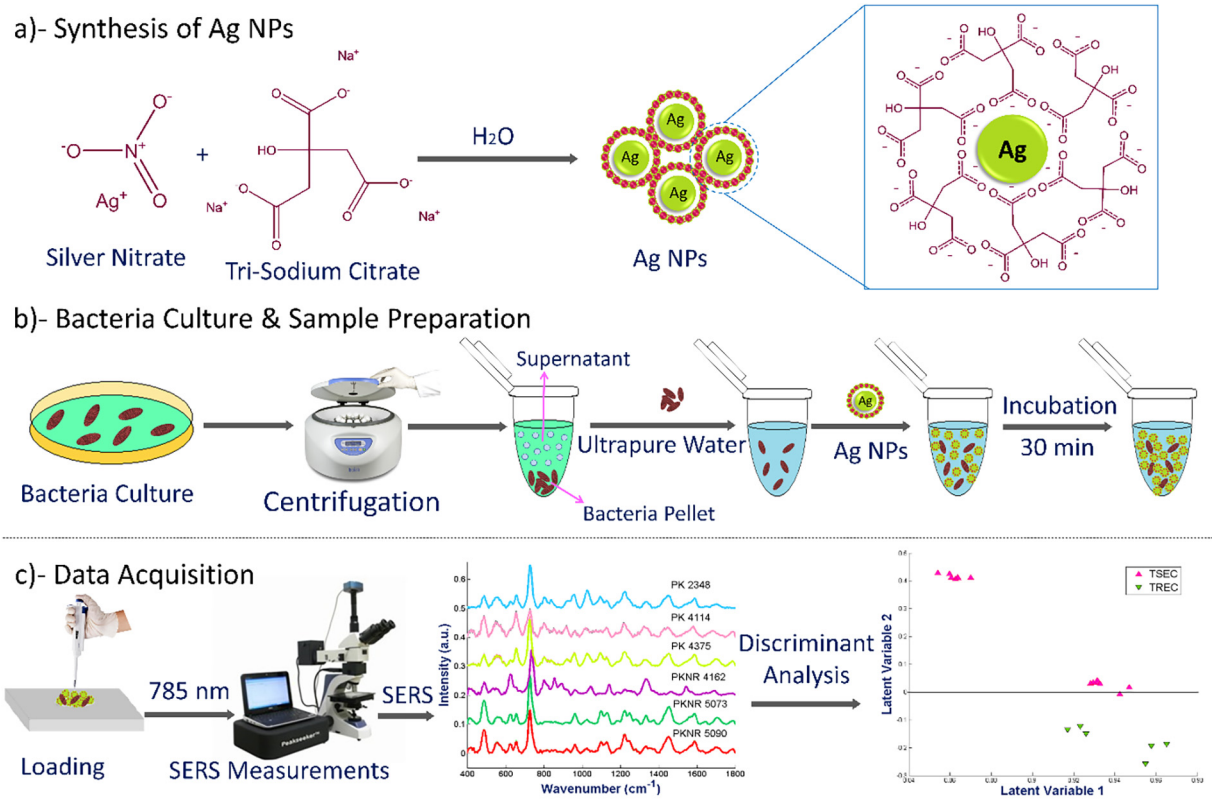


Fig. 1. Schematic representation for the SERS combining discriminant analysis technique showing (a) synthesis of Ag NPs (b) *E. coli* culturing and preparation of samples (c) SERS spectral acquisition with 785 nm laser light as an excitation source.

caused by the presence of different moieties and the presence of common fluorophores in biological species limits the use of photoluminescence and fluorescence techniques for bacterial identification [34,35]. Infrared (IR) spectroscopy can also be used to discriminate the different species of bacteria but its application is limited towards aqueous samples due to interference by water molecules [31].

Raman spectroscopy has been employed for the rapid detection and classification of microbes in an aqueous environment by providing their characteristic whole organism fingerprints corresponding to sample composition [33,36–38]. However, the weak intensity of the Raman signal can cause sample degradation due to high laser power and long spectral acquisition time [39]. Surface-enhanced Raman spectroscopy (SERS) has resolved the issues associated with Raman spectroscopy. In this technique, the intensity of the Raman signal is enhanced by keeping metallic nanoparticles or any roughened nanostructured metal surfaces in proximity to sample molecules causing a surface plasmon effect. SERS is the most promising method for the precise and rapid detection of antibiotic-resistant bacteria because it is a non-destructive, rapid, low-cost and highly sensitive technique [32,40–43].

The discovery of tet*(X3)*/*(X4)* has motivated scientists to develop a rapid detection method for tigecycline resistance in *E. coli*. Recently, TaqMan-based multiplex real-time PCR assay has been developed to distinguish the variants of *tet(X)* [44]. After that, the tetracycline inactivation method (TIM) based on microbial growth and matrix-assisted laser desorption ionization-time of flight mass spectrometry (MALDI-TOF MS) has been developed for the rapid detection of plasmid-mediated tigecycline resistance in *E. coli* and *Acinetobacter spp* [45,46]. To the best of our knowledge, there has been no report published yet for the surface-enhanced Raman spectroscopy based identification of *tet(X)*-producing *E. coli*. In the present study, the identification and differentiation of tigecycline-resistant *E. coli* (TREC) from tigecycline-sensitive *E. coli* (TSEC) has been performed by employing SERS and Ag NPs have been used as SERS substrate to enhance the Raman signal intensity by surface plasmon effect. The characteristic SERS vibrational features associated directly or indirectly with biochemical changes that occur due to tigecycline resistance have been identified by comparing the spectral data of all TREC and TSEC strains. Moreover, the identification algorithm of Principal Component Analysis (PCA) and clustering algorithm of Hierarchical cluster analysis (HCA) are used for the identification of TREC and TSEC *E. coli* strains and the successful discrimination among them has been achieved by Partial Least Square-Discriminant Analysis (PLS-DA).

2. Material and methods

2.1. Synthesis of silver nanoparticles (Ag NPs)

The chemical reduction method involving tri-sodium citrate ($Na_3C_6H_5O_7$) as both capping and reducing agent and silver nitrate ($AgNO_3$) as precursor was employed for the synthesis of Ag NPs that were used as a substrate in the SERS measurements. Briefly, 1 mM solution of silver nitrate was prepared by taking 200 ml of deionized water in a beaker and then 33.72 mg of $AgNO_3$ was added to it. The solution was heated until its boiling starts and then 1% $Na_3C_6H_5O_7$ solution was added to it followed by its further boiling at 600 rpm with continuous stirring for 1 h. After stopping heating, stirring was done to bring the solution to room temperature. The prepared grey-colored Ag NPs suspension was centrifuged for 7 min at 600 rpm to get the NPs by removing the supernatant [47].

2.2. Bacterial culture and sample preparation

2.2.1. E. Coli culturing

The 5 ml of Brain Heart Infusion broth in culture dishes were used as a medium for the culture of six different *E. coli* strains (PKNR 5090/5073/4162 and PK 4375/4114/2248) for 18 h at 37 °C followed by centrifugation at log phase for 10 min at 12000 rpm. As a result, the pellet of each strain separated from the supernatant and dissolved in 1.5 ml of sterilized phosphate-buffered saline (PBS). The Luria Bertani (LB) agar plate with the enumeration of these stock solutions in triplicate was incubated for 24 h at 37 °C to determine the concentration of bacteria in them.

2.2.2. Ag NPs-E.coli sample preparation

A volume of 50 µl of the prepared Ag NPs was mixed with 50 µl of each sample of *E. coli* strains in Eppendorf tube with the help of a micropipette and then kept at room temperature for an incubation time of 30 min so that there can be sufficient interaction between sample and nanoparticles for the better enhancement of the Raman signal.

2.3. Data acquisition

Raman spectrometer (ATR8300BS Optosky, China) equipped with an excitation source of 785 nm diode laser was used to record all SERS spectra. The aluminum slide with a small groove was used to hold the sample. The micropipette was used to transfer each incubated sample of all strains (50 µl drop) on the aluminum slide to acquire the SERS spectra. The sample was focused through 40 X/0.6 (N.A) objective lens of Amscope (MA 1000 model) attached with Raman spectrometer and then laser light of 120 mW power was used as Raman excitation light. To reduce the electrical noise, an air-cooled charged coupled detector (CCD) was employed. Seven spectra were acquired for every sample with an integration time of 20 sec. The reproducibility, stability, and robustness of our results were ensured by keeping all conditions for the SERS data acquisition constant.

2.4. Data Pre-Processing

The raw SERS spectral data of *E. coli* strains was imported into MATLAB® 7.8.0 R2009a (The MathWorks Inc., Natwick, MA, USA) for further preprocessing and data analysis. The SERS spectra were truncated in the range of 400–1800 cm^{-1}. The algorithms with in-house built script files of MATLAB® were applied for the smoothing, baseline correction, background removal, and normalization of the spectra. The SERS data of all strains was compiled into a single matrix and then the Savitzky-Golay filtering (S-G) with frame length 13 and polynomial order 3 was applied for smoothing the spectra followed by baseline correction in a rubberband fashion. Then, the same preprocessing was applied on an aluminum spectrum (background) and then it was subtracted from the spectra of all strains by minimizing a non-quadratic cost function. Finally, the vector normalization (VN) was applied [48,49].

2.5. Data analysis

The SERS signatures associated with tigecycline resistance in *E. coli* were identified by comparing the SERS spectral data of each TREC strain with each TSEC strain. The assignment and interpretation of all vibrational SERS bands is done based on literature [40,42,50–59] which are enlisted in Table 2. The relative standard deviation (RSD) was calculated to determine the reproducibility of

Table 2
SERS vibrational band assignments for all *E. coli* strains.

Peak assignments	Component	SERS shifts (cm^{-1})	References
C-O-C ring deformation, skeletal mode	Carbohydrates	488	[50,51]
Skeletal mode	Carbohydrates	554	[53]
Aromatic ring skeletal, Phenylalanine	Proteins	625	[53]
COO^- bending in tyrosine, guanine vibration	Amino acids/ Nucleic acids	656	[40,42,53,54,56,58]
Glycosidic ring vibrational mode (adenine, polyadenine, DNA)	Nucleic acids	727	[40,42,52–54]
Cytidine, uracil	Nucleic acids	785	[51]
Tyrosine, valine and porine (C-N stretching)	Proteins	803	[53,54]
Different C-N stretching in Tyrosine	Proteins	835–825	[80]
Tyrosine ring breathing	Proteins	854	[41,54]
Tryptophan	Proteins	893–881	
skeletal stretching (COO^-, C-C)	Proteins	919	[54]
C-N stretching, C = C deformation	Proteins	960	[42,53,54,56]
C-H deformation/adenine ring stretching	Proteins	1025	[55]
C-C ring breathing	Proteins	1044	[42,53]
C–O and C–C stretching, –C–OH bending	Carbohydrates	1095	[54,56,80]
Ring breathing, C-O-C stretching	Nucleic acids	1142–1128	[42,53]
C–C and C–H stretching	Lipids	1181	[81]
Adenine, polyadenine and DNA or Amide III	Nucleic acids / Proteins	1223	[53,54]
Amide III β sheet	Proteins	1246	[41,42,56]
Amide III (C-N-H deformation)	Proteins	1283	[58]
Adenine, polyadenine and DNA (NH_2 stretching)	Nucleic acids	1334–1320	[40,42,53,54]
COO^- stretching	Proteins	1376	[54,56]
CH_2 deformation	Lipids	1453	[42,54–56]
Amide II (C-N stretching, N-H bending)	Proteins	1545	[53]
CH_2 deformation		1559	[80]
Ring stretching (Adenine, guanine)	Nucleic acids	1588	[42,54,56,59]
Amide I α-helix	Proteins	1710–1642	[42,54,57,58 56]

the results. The hidden information between variables is detected efficiently and effectively by using different tools including PCA, HCA, and PLS-DA for multivariate data analysis over the entire spectral range of 400–1800 cm^{-1}. The qualitative analysis of data was performed by PCA which is a dimensionality reduction tool that converts a larger number of original variables (correlated variables) into a smaller number of principal components (uncorrelated variables) containing all the useful information without using any prior information of samples because it is an unsupervised learning algorithm [60]. PCA develops a new coordinate system to reduce the complexity of data in which new orthogonal vectors (basis sets) are made by a linear transformation of the original spectra that are considered as N-dimensional vectors where a total number of data points in one spectrum is indicated by N. Total number of spectra of all samples (X) are compiled in a single matrix which is decomposed into loadings (P) and scores (T) in smaller matrices ($X = TP^T + E$). The multiplication of loadings and scores of each spectrum cannot explain some information that is known as residual and indicated by E. The important principal components (PCs) are selected based on their percentage of variance explained in a multi-dimensional dataset. The similarity in the features of spectra is revealed by plotting the PCA scores in clusters and the reason for the variability in the SERS spectral data of different *E. coli* strains are explained by extracting the PC loadings (diagnostic vibrations) that are the orthogonal dimensions of the data [61,62].

Moreover, Unscrambler® X 10.4 software (CAMO, Oslo, Norway) was used for HCA that is another qualitative analysis used to improve the clustering of the SERS spectral data. The dendrogram is a graphical representation of HCA that is built based on a hierarchy of clusters and sub-clusters that have been formed based on the resemblances in the data. Ward's method, a minimum variance method, is used for HCA that merges the most similar cluster pair resulting in a minimum total error sum of squares (TSS) within the group. Furthermore, a discriminant analysis, PLS-DA, was performed to differentiate the SERS spectral data of TREC and TSEC strains. As compared to PCA, it is a supervised modeling technique that uses the previous information of classes as y-variable against spectral data as **x**-variable. The sensitivity, specificity, accuracy, and area under receiver operating characteristic (AUROC) were calculated to check the efficiency and performance of the model that was built on binary classification between spectra of TREC and TSEC strains.

3. Results and discussion

3.1. Mean spectra

In the current study, Ag NPs have been used as SERS substrate to enhance the Raman signal. The strong surface plasmon properties of gold (Au) and silver NPs have equipped them with the highest SERS enhancement factor. Ag NPs have been extensively used in several studies as an active substrate for the SERS analysis of different bacteria [63–69]. As compared to Au NPs, the SERS enhancement is stronger with Ag NPs because of the enhanced surface plasmon resonance due to a greater number of active sites (hotspots). Additionally, they are easy to prepare, cheap, and have a high molar extinction coefficient [68,70]. Ag NPs show antibacterial activity which depends on their size, shape, aggregation, type of bacteria, environmental conditions, generation of reactive oxygen species (ROS), and surface coatings [71–76]. Their antibacterial activity decrease with decreasing the concentration of Ag NPs and increasing the particle size of Ag NPs. Spherical Ag NPs show limited activity as compared to plate-shaped Ag NPs [77,78]. We have prepared Ag NPs with the previous protocol used in our recent publication and their TEM characterization has shown that they are spherical in shape with an average diameter of 53 nm that indicates their limited antimicrobial activity [79].

All spectra of six strains have been pre-processed to extract the useful information and then the mean was taken for seven spectra of every strain and they have been shown in the mean spectra plot. The average/mean is very important in statistics to find the central

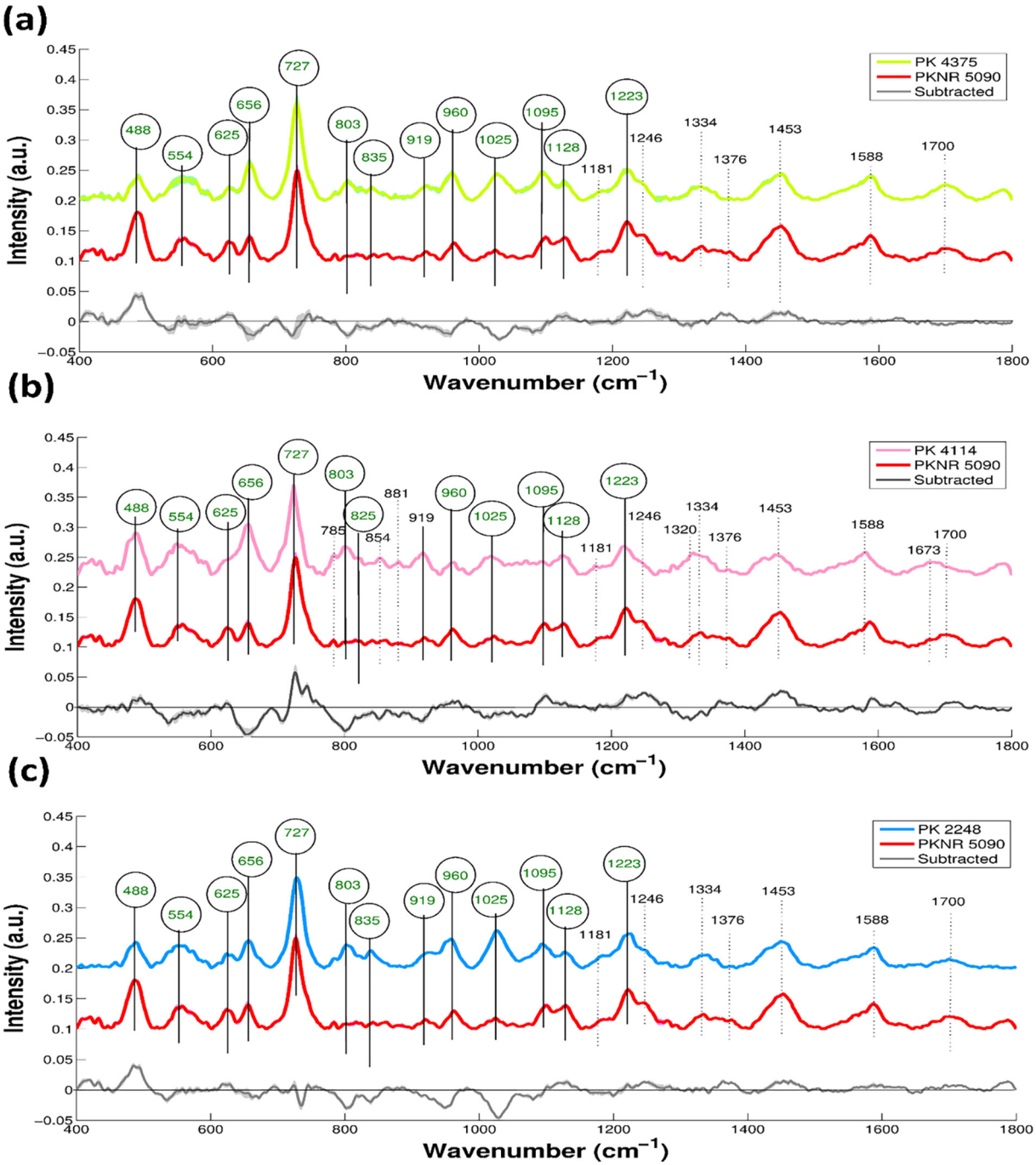


Fig. 2. Comparison of SERS spectra of PKNR 5090 TSEC strain with all SERS spectra of TREC strains (a) PK 4375 (b) PK 4114 (c) PK 2248.

tendency of all the datasets for each strain. Figs. 2, 3, and 4 show the comparison between the mean spectra of all TSEC and TREC strains. Every mean spectrum of TSEC has been plotted against each mean spectrum of TREC to identify and confirm the unique features that are specifically associated with the tigecycline resistance development in *E. coli*. The reproducibility in the SERS measurements was checked by calculating the relative standard deviation (RSD) that was found to be less than 10% for all *E. coli* strains.

The vertical lines have been drawn for all the SERS spectral features of different *E. coli* strains appeared due to biochemical changes mainly in the cell wall components of bacteria including carbohydrates, proteins, lipids, and polysaccharides [68]. These features are compared with known SERS spectra of biological molecules and have been enlisted in Table 2. The cell wall of gram-negative bacteria such as *E. coli* has greater protein content than gram-positive bacteria hence the band at 1330 cm^{-1} appears only in gram-negative bacteria [82]. The adenine, polyadenine, or adenosine monophosphate (AMP) of bacterial DNA give SERS signal at 1332 cm^{-1} and intense SERS signal at 730 cm^{-1} [32,83,84]. The bands that appear at 488 cm^{-1} and 554 cm^{-1} are assigned to C-O-C ring deformation and skeletal modes of carbohydrates [50]. The region of 1220–1290 belongs to amide III that indicates the rich protein content in samples [51]. The SERS features of bacteria are mostly associated with vibrational modes of cell wall components including lipids, nucleic acids, membrane proteins/lipopolysaccharides, and peptidoglycan [54,85] and the metabolites of purine

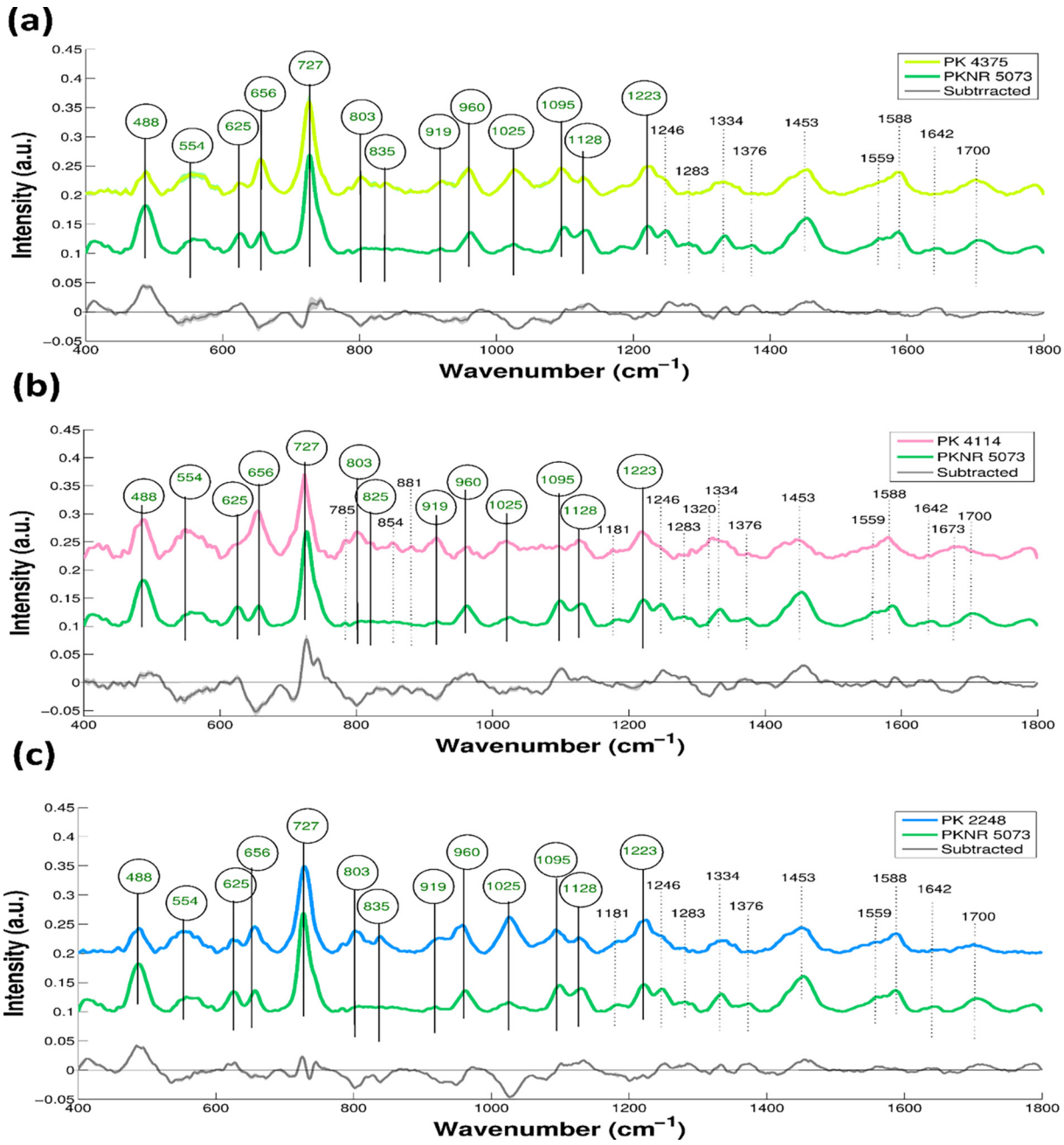


Fig. 3. Comparison of SERS spectra of PKNR 5073 TSEC strain with all SERS spectra of TREC strains (a) PK 4375 (b) PK 4114 (c) PK 2248.

degradation such as adenine, AMP, xanthine, hypoxanthine, uric acid, and guanine [86]. Live bacteria constantly excrete purine derivatives [87]. The prominent peak at 727 cm^{-1} and a weak band at 1334–1320 cm^{-1} are related to ring breathing mode of purine and ring vibrational mode of adenine and related components and they also indicate a close binding between cell wall of bacteria and SERS-active substrate (Ag NPs). The peak at 727 cm^{-1} also corresponds to flavin-bearing molecules such as nicotinamide adenine dinucleotide (NAD) and flavin adenine dinucleotide (FAD) which play an important role in the cellular respiration of the bacterial cell membrane. The presence of a prominent band at 727 cm^{-1} in all strains shows no disrupted purine mechanism [67,88,89] that indicates that a limited antibacterial activity of these Ag NPs have not effected SERS features of bacteria.

The SERS features associated with tigecycline resistance development in *E. coli* have been identified by comparing each SERS spectra of TSEC with each SERS spectra of TREC strain The spectral changes that are consistent in all six pair comparison spectra associated with the development of tigecycline resistance are marked at 488 cm^{-1}, 554 cm^{-1}, 625 cm^{-1}, 656 cm^{-1}, 727 cm^{-1},803 cm^{-1}, 825–835 cm^{-1}, 919 cm^{-1}, 960 cm^{-1}, 1025 cm^{-1}, 1095 cm^{-1}, 1128 cm^{-1}, and 1223 cm^{-1} that are associated with proteins, nucleic acids, and carbohydrates and have been indicated by solid lines. The SERS band at 488 cm^{-1} appear due to C-O-C ring deformation, 554 cm^{-1} due to skeletal mode of carbohydrates, 625 cm^{-1} due to aromatic ring skeletal mode of phenylalanine, 656 cm^{-1} due to guanine vibration or stretching mode of carboxylate in amino acids, 727 cm^{-1} due to glycosidic ring mode of DNA and adenine

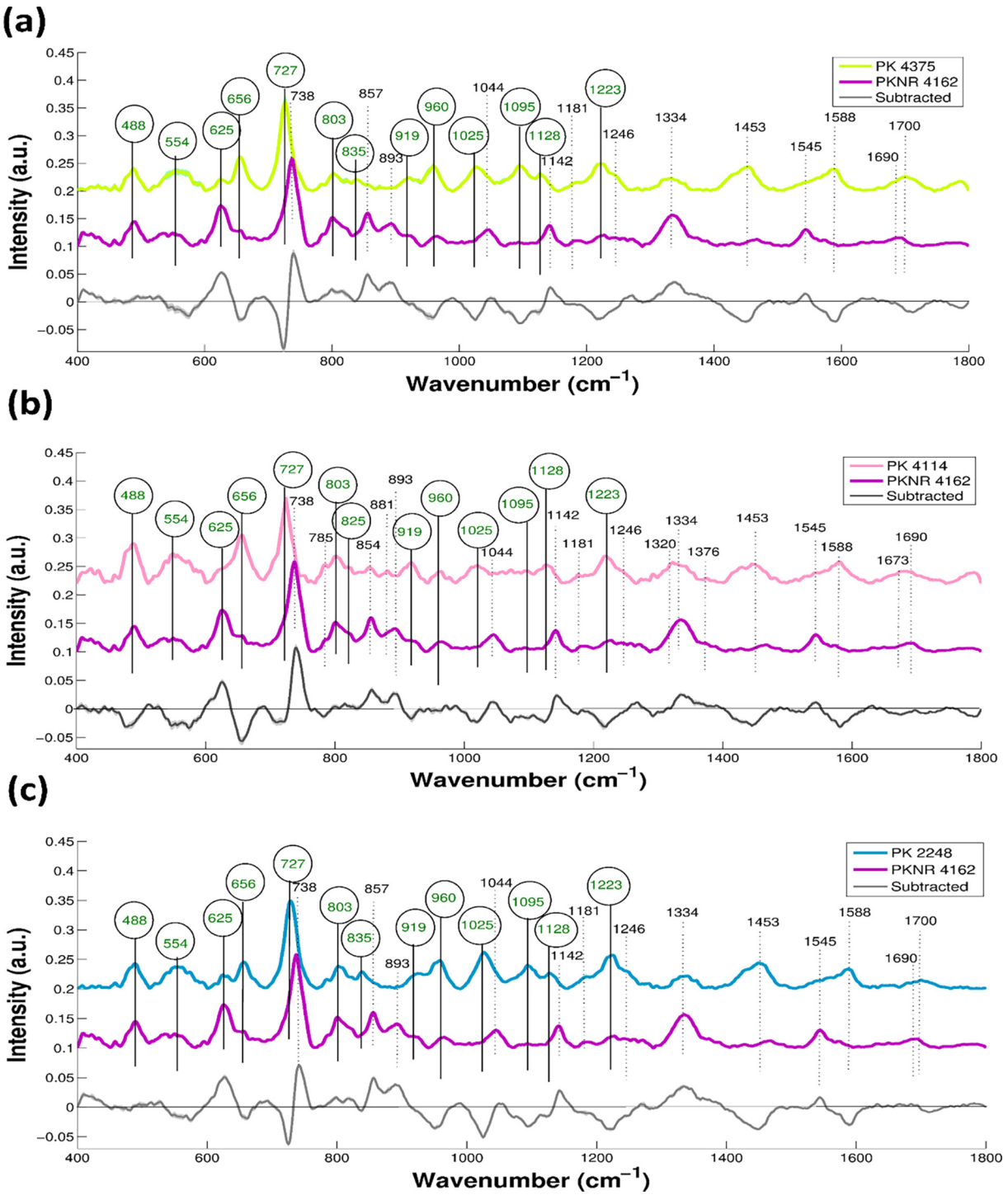


Fig. 4. Comparison of SERS spectra of PKNR 4162 TSEC strain with all SERS spectra of TREC strains (a) PK 4375 (b) PK 4114 (c) PK 2248.

and polyadenine in FAD and NAD, 803 cm^{-1} due to C-N stretching of amino acids,825–835 cm^{-1} due to different C-N stretching in tyrosine, 919 cm^{-1} due to C–C and carboxylate skeletal stretching in proteins, 960 cm^{-1} due to C-N stretching and C = C deformation, 1025 cm^{-1} due to C–H deformation or adenine ring stretching, 1095 cm^{-1} due to C–O and C–C stretching and –C–OH bending, 1128 cm^{-1} due to C-O-C stretching and ring breathing and 1223 cm^{-1} due to amide III or adenine, polyadenine, and DNA.

The TREC strains harbour *tet(X)* gene encoding for TetX protein which is a flavin-dependent monooxygenase (FMO) causing tigecycline resistance in *E. coli*. FMO (TetX) can hydroxylate tigecycline regioselectively into an unstable compound (11a-hydroxytigecycline) that undergoes decomposition limiting the antibacterial activity of tigecycline. The presence of O_2, nicotinamide adenine dinucleotide phosphate (NADPH), Mg^{2+} is required for this TetX-catalysed hydroxylation[21,90]. The bands at 803 cm^{-1} (C-N stretching in tyrosine, valine, and porine) and 825–835 cm^{-1} (different C-N stretching in tyrosine) are present in only TREC strains. In all the TREC strains, the intensity of the peak at 488 cm^{-1} (C-O-C ring deformation) and 625 cm^{-1}

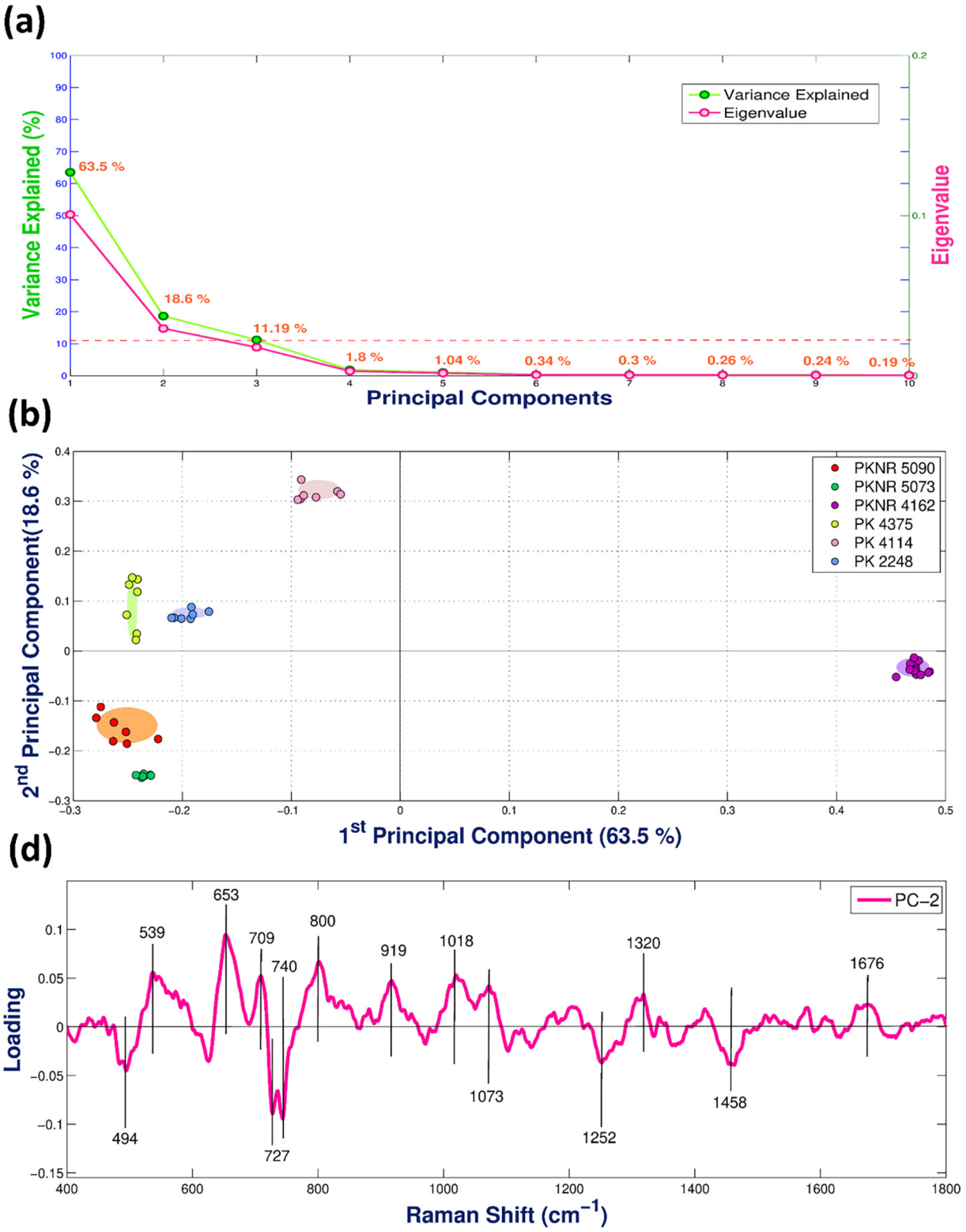


Fig. 5. (a) Scree plot for first ten PCs along x-axis against the percentage of explained variance on the left y-axis and eigenvalues on the right y-axis (b) scores plot between first two PCs for PCA performed for all *E. coli* strains (c) loading plot of PC-2 for PCA performed on all six strains against wavenumbers.

(aromatic ring skeletal mode in phenylalanine) is decreased and at 656 cm^{-1} (guanine vibration, stretching mode of carboxylate in tyrosine) and 919 cm^{-1} (COO^{-} and C-C skeletal stretching) is increased as compared to all TSEC strains increased due to protein-rich content indicating the development of tigecycline resistance in TREC strains. There is a high-intensity broad peak in all TREC strains at 554 cm^{-1} (skeletal mode vibration of carbohydrates). There are random or irregular changes at 727 cm^{-1}, 1025 cm^{-1}, 1095 cm^{-1}, 1128 cm^{-1}, and 1223 cm^{-1} between TSEC and TREC strains. Although the PKNR 4162 is a TSEC strain, it

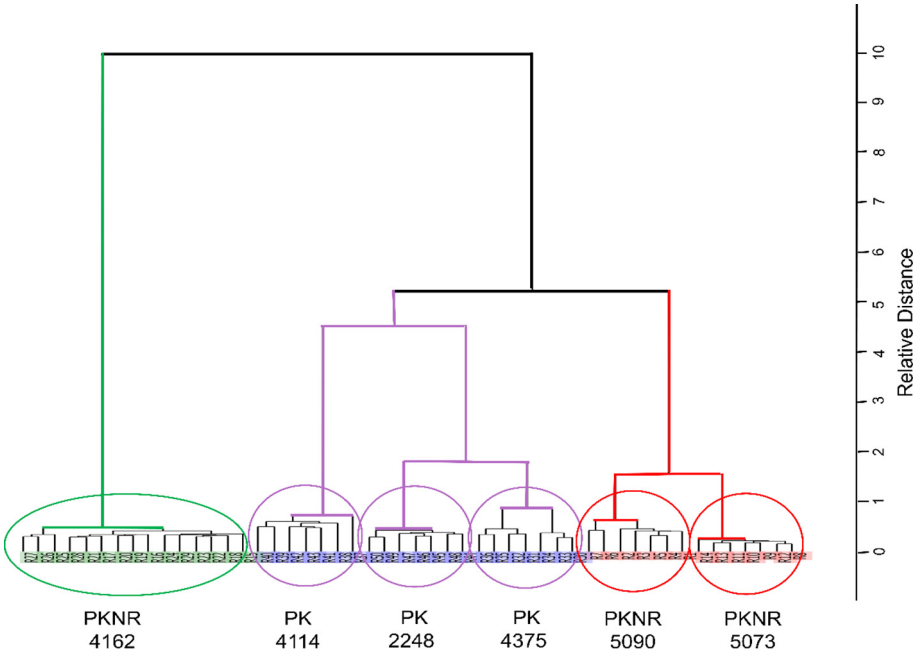


Fig. 6. HCA dendrogram showing a hierarchy of all *E. coli* strains based on the similarity in their features.

shows resistance against carbapenems due to which this strain is showing some exceptional behavior than other TSEC strains such as the presence of bands at 803 cm^{-1} and 825 cm^{-1} and the decreased band intensity at 488 cm^{-1}.

SERS is a potential technique that can be employed to differentiate bacteria at the strain level. Although all *E. coli* strains used in this study belong to only one specie, they show some similarities in their SERS spectra and many resembling SERS features can be seen among three TREC strains as well as three TSEC strains because of their similar behavior towards tigecycline, the individual strains can be distinguished from each other because every strain possesses a characteristic SERS spectrum. All *E. coli* strains have a weak signal at 1181 cm^{-1} and a weak broad peak for amide-I also appeared for all strains at 1700 cm^{-1} that is little shifted to 1690 cm^{-1} for PKNR 4162 and 1673 cm^{-1} for PK 4114. The two TSEC strains (PKNR 5090 and PKNR 5073) have a common strain-specific feature at 1376 cm^{-1} (carboxylate stretching) that is absent in all other *E. coli* strains. There are additional strain-specific features present in *E. coli* strains such as a very weak broad band at 1283 cm^{-1} (C-N-H deformation in amide III) and 1642 cm^{-1} (Amide I α-helix) and a weak shoulder at 1559 cm^{-1} is present in SERS spectra of PKNR 5073 strain. Moreover, the PK 4114 strain has specific features at 785 cm^{-1} (Cytidine, uracil), 854 cm^{-1} (ring breathing in tyrosine), 881 cm^{-1} (tryptophan), and there is a shifting of a band at 1334 cm^{-1} to 1320 cm^{-1} (NH_2 stretching in adenine, polyadenine, and DNA).

The carbapenem-resistant and tigecycline-sensitive PKNR 4162 strain shows greater variability to all other strains because it has a large number of additional features at 857 cm^{-1} (tyrosine ring breathing), 893 cm^{-1} (tryptophan), 1044 cm^{-1} (C-C ring breathing), 1142 cm^{-1} (C-O-C stretching and ring breathing,) and 1545 cm^{-1} (C-N stretching, and N-H bending in amide II). The band at 727 cm^{-1} is shifted to 738 cm^{-1} and the band at 1700 cm^{-1} has appeared at 1690 cm^{-1} in this strain. Notably, the peaks at 1223 cm^{-1} and 1588 cm^{-1} and a low-intensity shoulder at 1246 cm^{-1} appear for all other strains but absent in the PKNR 4162 strain. Some of these unique changes in the SERS spectra of this strain may be due to carbapenem resistance development and some can be unique features of this strain.

3.2. Principal Component analysis (PCA)

The potential of SERS is checked by performing PCA for the rapid and reproducible identification of different *E. coli* strains and the differentiation of TREC and TSEC strains. The dimensions of the original multi-dimensional datasets are reduced by PCA to minimize the complexity in data and transformed into new variables that are orthogonal to each other and known as principal components (PCs). The identical spectra can be accurately differentiated by PCA due to its ability to highlight minor spectral differences. After applying pre-treatment methods on raw data, the algorithm of singular value decomposition (SVD) is used to decompose the original variables into loadings, scores, and eigenvalues. The important PCs are selected based on eigenvalues and explained variance. The PCs have both eigenvalues and explained variance in descending order in which PC-1 always has the highest values followed by decreasing values for other PCs. The PCs with the lowest percentage of explained variance or smaller eigenvalues provide no useful information regarding data and are hence eliminated. The eigenvalues and explained variance have been plotted against the first 10 PCs in the scree plot as shown in Fig. 5 **(a)**. In the current study, the maximum variability in the data is explained by the first three PCs that accounts for 93.3% of the total explained variance and all other PCs were ignored. The maximum features containing useful information for the differentiation of TSEC and TREC strains and inter-strain level differences can be explained by them.

The changes in the SERS vibrational fingerprints are analysed by plotting the scores and loadings for the dominant PCs. The scores for the PC-1 and PC-2 have been plotted in 2D scatter plot with a 95% confidence interval error eclipses (Fig. 5 **(b)**). The 63.5% and 18.6% of the variance are explained by PC-1 and PC-2 respectively. The strains are well-differentiated along with both components. The SERS spectral data of PKNR 4162 strain (TSEC) is clustered on the positive side of PC-1 while spectra of all other five TSEC and TREC strains are clustered on the negative side of PC-2 indicating that this strain is greatly variant from all other strains based on its SERS fingerprints. As we already know, PKNR 4162 is resistant to carbapenem antibiotics which is the reason for its variability compared to the other two TSEC strains. The main discriminant

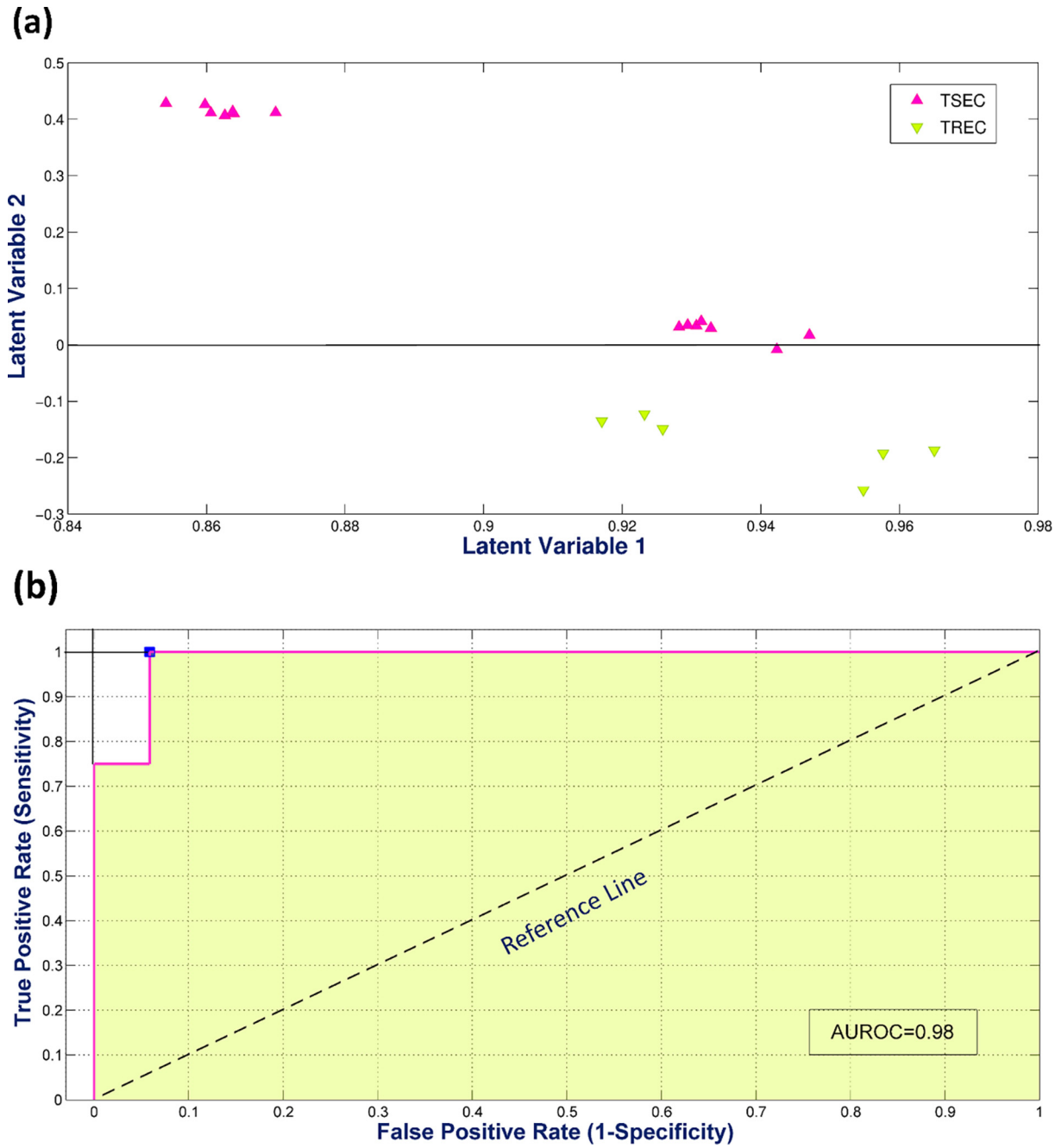


Fig. 7. (a) Scores plot for the test dataset of all *E. coli* strains by PLS-DA (b) Approach of ROC curve with the optimal operating point (blue circle) for checking the performance of PLS-DA model for different TREC and TSEC strains.

for the differentiation of TREC and TSEC strains is PC-2 because it has clearly clustered spectral data sets of TREC on the positive side and TSEC strains on the negative side irrespective of the fact that PC-1 explains the maximum variance.

The analysis of PCA scores gives an idea about the variability in our data in the form of visual representation of different groupings/clusters but it does not provide any information regarding the reason for the variability in the data that separates the data in the form of different clusters. The underlying relationship in the original variables is determined by performing the PCA loadings analysis. Loadings could be described as a vector of correlation coefficients with each principal component score between variables of the original dataset. This gives insight into particular features that contribute significantly to the clustering of spectra. The high positive or negative loadings of a variable make it useful for the diagnostic purpose because they play a major role in the data variability with respective PC as compared to other variables. As we can see in Fig. 5 **(b)**, only PKNR 4162 strain is present on the positive axis while all other strains are present on the negative side so the loadings plot of PC-1 cannot give useful information regarding features that give a significant contribution in the differentiation of TREC and TSEC strains. The scores of PC-2 have differentiated TREC and TSEC strains so the loadings plot of PC-2 can be used to determine the features belonging to TREC or TSEC strains. The loadings plot of PC-2 has been plotted against wavenumbers (variables) to get the significant diagnostic information as shown in Fig. 5 **(c)**. The weight of discrimination among *E. coli* strains is heavy at SERS vibrational bands of 494 cm^{-1},

539 cm^{-1}, 653 cm^{-1}, 709 cm^{-1}, 727 cm^{-1}, 740 cm^{-1}, 800 cm^{-1}, 919 cm^{-1}, 1018 cm^{-1}, 1073 cm^{-1}, 1252 cm^{-1}, 1320 cm^{-1}, 1458 cm^{-1} and 1676 cm^{-1}. The bands related to TREC strains are found at 653 cm^{-1} (guanine vibration or COO^- bending in tyrosine), 800 cm^{-1} (C-N stretching in amino acids), 919 cm^{-1} (skeletal stretching in proteins), and 1020 cm^{-1} (C-H deformation) and the bands linked to TSEC are observed at 494 cm^{-1} (C-O-C ring deformation and skeletal mode of carbohydrates), 727 cm^{-1} (glycosidic ring vibrational mode of adenine and polyadenine), 1252 cm^{-1} (amide III) and 1458 cm^{-1} (CH_2 deformation) out of the SERS vibrational features associated with tigecycline resistance have been identified in mean SERS spectra. Due to band shifting of 727 cm^{-1} to 738 cm^{-1} in PKNR 4162 strain (Fig. 4), a band can be seen at 1740 cm^{-1} along with 1727 cm^{-1}. In addition, some other strain-specific features are also observed. These findings are compatible with the mean spectra and show the ability of SERS as a label-free rapid and reproducible method to differentiate between SERS spectral data of various TREC and TSEC strains.

3.3. Hierarchal cluster analysis (HCA)

The chemical or physical interpretation of multi-dimensional data is not disclosed by PCA because it offers only a visual representation of widely spread data in the form of clusters. Similar to identification algorithm (PCA), clustering algorithms also do not require any previous knowledge of classes. HCA algorithm was applied to data to construct a dendrogram that shows the hierarchy of data in the form of clusters and sub-clusters based on the similarity in data. The algorithm of Ward's method was used to generate a dendrogram over the entire spectral range of 400–1800 cm^{-1} that was based on Squared Euclidean distance. Ward's clustering method is based on merging the pair of clusters that contain the most similar information to provide the minimum increase in the total error sum of squares (TESS) within a group.

According to Ward's method, a total number of spectra of all *E.-coli* strains are first assembled into an equal number of clusters containing a single spectrum in a single cluster and then the number of clusters is reduced by linking the most similar pair of clusters that reduces within-group TESS. All clusters are merged following these steps. Fig. 6 shows three major clusters in which three strains of TREC are assembled in the first cluster (purple), two strains of TSEC are assembled in the second cluster (red) and the third cluster (green) is based on a single strain of TSEC (PKNR 4162) which is a carbapenem-resistant strain. Similar to PCA, this strain shows a greater amount of variability from the other two strains of TSEC because of its resistance towards carbapenem antibiotics. Three clusters have mainly six sub-clusters that show the potential of the SERS technique to differentiate the bacteria at the strain level. Out of three TREC strains, two of them (PK 4375 and PK 2248) match well each other because they share additional common strain-specific SERS feature at 1700 cm^{-1} while PK 4114 is showing a little variability due to a greater number of strain-specific SERS features belong to this strain and shifting of 1700 cm^{-1} peak to 1673 cm^{-1}.

3.4. Discriminant analysis

The inspection of scores of both PCA and HCA provides only visual differentiation of all *E. coli* strains and fails to provide any quantitative information regarding data. The discriminant analysis such as PLS-DA is based on both partial least squares analysis (PLS) and linear discriminant analysis (LDA). PLS-DA is a supervised classification modeling algorithm used for the quantitative discrimination among TREC and TSEC strains by using the prior information of classes. All data is compiled into a matrix followed by its randomization to remove biasedness in results. After that, the data is split independently into a 60% calibration dataset and a 40% validation dataset.

The Bayes theorem was used to build or fit the model on the calibration dataset along with cross-validation (Montecarlo). To achieve a large accuracy in results, the variables providing the lowest prediction error are extracted and considered as optimal latent variables (LVs). The cross-validation provided fourteen (14) optimal LVs in this study which were used to train the PLS-DA model on the calibration dataset. The trained model was then applied to the validation dataset to check the performance of the model because this dataset was kept independent from the model training process. The scores of PLS-DA have been plotted in Fig. 7 **(a)** indicating a clear differentiation among TREC and TSEC strains without any wrong prediction with 100% sensitivity, 98.7% specificity, and 100% accuracy that shows the best performance of this model. To check the diagnostic potential of SERS and the effectiveness and performance of the PLS-DA classification model, the receiver operating characteristic (ROC) curve was also plotted, as shown in Fig. 7 **(b)**. Between 1-specificity (false positive rate) and sensitivity (the true positive rate) and, the ROC curve was mapped. The model's excellent efficiency is indicated by the value of AUROC which is 0.98. The PLS-DA has classified TREC and TSEC strains in a better way as compared to identification (PCA) and clustering analysis (HCA).

4. Conclusions

Surface-enhanced Raman spectroscopy combining discriminant analysis has the potential for the rapid and reproducible identification and discrimination of TREC strains from TSEC strains. Silver nanoparticles have been employed as SERS substrate to enhance the Raman signal. The comparison of the SERS spectral data sets of each TREC strain against the TSEC strain provided unique and characteristic features that belong to tigecycline resistance in different *E. coli* strains. This technique has also discriminated individual strains from each other comprising specific features for each strain. The different *E. coli* strains have been differentiated in the form of clusters by different chemometric tools including PCA and HCA. The successful discrimination among two classes of TREC and TSEC strains has been performed by a supervised classification algorithm called PLS-DA with 98% AUROC curve, 100% sensitivity, 98.7% specificity, and 100% accuracy.

CRediT authorship contribution statement

Saba Bashir: Writing - original draft. **Haq Nawaz:** Conceptualization, Supervision, Project administration, Validation. **Muhammad Irfan Majeed:** Writing - review & editing, Validation. **Mashkoor Mohsin:** Conceptualization, Writing - review & editing, Validation. **Ali Nawaz:** Formal analysis. **Nosheen Rashid:** Conceptualization, Writing - review & editing, Validation. **Fatima Batool:** Writing - review & editing. **Saba Akbar:** Software. **Muhammad Abubakar:** Formal analysis. **Shamsheer Ahmad:** Formal analysis. **Saqib Ali:** Conceptualization, Resources. **Muhammad Kashif:** Data curation.

Declaration of Competing Interest

The authors have no known competing financial interests or personal relationships that could have appeared to influence the work reported in this paper.

Acknowledgements

This work was supported by the Higher Education Commission (HEC) of Pakistan [Grants 8494/NRPU & 6400/NRPU].

References

[1] Y. Sun, Y. Cai, X. Liu, N. Bai, B. Liang, R. Wang, The emergence of clinical resistance to tigecycline, International Journal of Antimicrobial Agents 41 (2013) 110–116.
[2] T. Hirata, A. Saito, K. Nishino, N. Tamura, A. Yamaguchi, Effects of efflux transporter genes on susceptibility of Escherichia coli to tigecycline, GAR-936, Antimicrobial agents and chemotherapy 48 (2004) 2179–2184.
[3] D.M. Livermore, Tigecycline: what is it, and where should it be used?, Journal of Antimicrobial Chemotherapy 56 (2005) 611–614.
[4] P.J. Petersen, N. Jacobus, W. Weiss, P. Sum, R. Testa, In vitro and in vivo antibacterial activities of a novel glycylcycline, the 9-t-butylglycylamido derivative of minocycline, GAR-936, Antimicrobial agents and chemotherapy 43 (1999) 738–744.
[5] G.E. Stein, T. Babinchak, Tigecycline: an update, Diagnostic Microbiology and Infectious Disease 75 (2013) 331–336.
[6] K.K. Kumarasamy, M.A. Toleman, T.R. Walsh, J. Bagaria, F. Butt, R. Balakrishnan, U. Chaudhary, M. Doumith, C.G. Giske, S. Irfan, P. Krishnan, A.V. Kumar, S. Maharjan, S. Mushtaq, T. Noorie, D.L. Paterson, A. Pearson, C. Perry, R. Pike, B. Rao, U. Ray, J.B. Sarma, M. Sharma, E. Sheridan, M.A. Thirunarayan, J. Turton, S. Upadhyay, M. Warner, W. Welfare, D.M. Livermore, N. Woodford, Emergence of a new antibiotic resistance mechanism in India, Pakistan, and the UK: a molecular, biological, and epidemiological study, The Lancet Infectious Diseases 10 (2010) 597–602.
[7] G.A. Noskin, Tigecycline: a new glycylcycline for treatment of serious infections, Clinical infectious diseases 41 (2005) S303–S314.
[8] J. Sun, C. Chen, C.-Y. Cui, Y. Zhang, X. Liu, Z.-H. Cui, X.-Y. Ma, Y. Feng, L.-X. Fang, X.-L. Lian, Plasmid-encoded tet (X) genes that confer high-level tigecycline resistance in Escherichia coli, Nature microbiology 4 (2019) 1457–1464.
[9] T. He, R. Wang, D. Liu, T.R. Walsh, R. Zhang, Y. Lv, Y. Ke, Q. Ji, R. Wei, Z. Liu, Emergence of plasmid-mediated high-level tigecycline resistance genes in animals and humans, Nature microbiology 4 (2019) 1450–1456.
[10] D.G. Guiney Jr, P. Hasegawa, C.E. Davis, Expression in Escherichia coli of cryptic tetracycline resistance genes from Bacteroides R plasmids, Plasmid 11 (1984) 248–252.
[11] S. Ghosh, T.M. LaPara, The effects of subtherapeutic antibiotic use in farm animals on the proliferation and persistence of antibiotic resistance among soil bacteria, The ISME journal 1 (2007) 191–203.
[12] T.A. Leski, U. Bangura, D.H. Jimmy, R. Ansumana, S.E. Lizewski, D.A. Stenger, C. R. Taitt, G.J. Vora, Multidrug-resistant tet (X)-containing hospital isolates in Sierra Leone, International journal of antimicrobial agents 42 (2013) 83–86.
[13] Y. Zeng, N. Dong, R. Zhang, C. Liu, Q. Sun, J. Lu, L. Shu, Q. Cheng, E.-W.-C. Chan, S. Chen, Emergence of an Empedobacter falsenii strain harbouring a tet (X)-variant-bearing novel plasmid conferring resistance to tigecycline, Journal of Antimicrobial Chemotherapy 75 (2020) 531–536.
[14] D. He, L. Wang, S. Zhao, L. Liu, J. Liu, G. Hu, Y. Pan, A novel tigecycline resistance gene, tet (X6), on an SXT/R391 integrative and conjugative element in a Proteus genomospecies 6 isolate of retail meat origin, Journal of Antimicrobial Chemotherapy 75 (2020) 1159–1164.
[15] A.J. Gasparrini, J.L. Markley, H. Kumar, B. Wang, L. Fang, S. Irum, C.T. Symister, M. Wallace, C.-A.-D. Burnham, S. Andleeb, Tetracycline-inactivating enzymes from environmental, human commensal, and pathogenic bacteria cause broad-spectrum tetracycline resistance, Communications biology 3 (2020) 1–12.
[16] L. Wang, D. Liu, Y. Lv, L. Cui, Y. Li, T. Li, H. Song, Y. Hao, J. Shen, Y. Wang, Novel plasmid-mediated tet (X5) gene conferring resistance to tigecycline, Eravacycline, and Omadacycline in a clinical Acinetobacter baumannii isolate, Antimicrobial Agents and Chemotherapy 64 (2019).
[17] Q. Chen, X. Li, H. Zhou, Y. Jiang, Y. Chen, X. Hua, Y. Yu, Decreased susceptibility to tigecycline in Acinetobacter baumannii mediated by a mutation in trm encoding SAM-dependent methyltransferase, Journal of Antimicrobial Chemotherapy 69 (2013) 72–76.
[18] X. Li, L. Liu, J. Ji, Q. Chen, X. Hua, Y. Jiang, Y. Feng, Y. Yu, Tigecycline resistance in Acinetobacter baumannii mediated by frameshift mutation in plsC, encoding 1-acyl-sn-glycerol-3-phosphate acyltransferase, European Journal of Clinical Microbiology & Infectious Diseases 34 (2015) 625–631.
[19] V. Cattoir, C. Isnard, T. Cosquer, A. Odhiambo, F. Bucquet, F. Guérin, J.-C. Giard, Genomic analysis of reduced susceptibility to tigecycline in Enterococcus faecium, Antimicrobial agents and chemotherapy 59 (2015) 239–244.
[20] L. Villa, C. Feudi, D. Fortini, A. García-Fernández, A. Carattoli, Genomics of KPC-producing Klebsiella pneumoniae sequence type 512 clone highlights the role of RamR and ribosomal S10 protein mutations in conferring tigecycline resistance, Antimicrobial agents and chemotherapy 58 (2014) 1707–1712.
[21] I.F. Moore, D.W. Hughes, G.D. Wright, Tigecycline is modified by the flavin-dependent monooxygenase TetX, Biochemistry 44 (2005) 11829–11835.
[22] A. Ruzin, D. Keeney, P.A. Bradford, AdeABC multidrug efflux pump is associated with decreased susceptibility to tigecycline in Acinetobacter calcoaceticus–Acinetobacter baumannii complex, Journal of Antimicrobial Chemotherapy 59 (2007) 1001–1004.
[23] F. McAleese, P. Petersen, A. Ruzin, P.M. Dunman, E. Murphy, S.J. Projan, P.A. Bradford, A novel MATE family efflux pump contributes to the reduced susceptibility of laboratory-derived Staphylococcus aureus mutants to tigecycline, Antimicrobial agents and chemotherapy 49 (2005) 1865–1871.
[24] F.R. Madiyar, S. Bhana, L.Z. Swisher, C.T. Culbertson, X. Huang, J. Li, Integration of a nanostructured dielectrophoretic device and a surface-enhanced Raman probe for highly sensitive rapid bacteria detection, Nanoscale 7 (2015) 3726–3736.
[25] L.E. Lehmann, K.-P. Hunfeld, T. Emrich, G. Haberhausen, H. Wissing, A. Hoeft, F. Stüber, A multiplex real-time PCR assay for rapid detection and differentiation of 25 bacterial and fungal pathogens from whole blood samples, Medical microbiology and immunology 197 (2008) 313–324.
[26] L. Zhu, J. He, X. Cao, K. Huang, Y. Luo, W. Xu, Development of a double-antibody sandwich ELISA for rapid detection of Bacillus Cereus in food, Scientific Reports 6 (2016) 1–10.
[27] S. Sauer, M. Kliem, Mass spectrometry tools for the classification and identification of bacteria, Nature Reviews Microbiology 8 (2010) 74–82.
[28] R. Jiang, H. Chen, L. Shao, Q. Li, J. Wang, Unraveling the evolution and nature of the plasmons in (Au core)–(Ag shell) nanorods, Advanced Materials, 24 (2012) OP200-OP207.
[29] D. Cheng, M. Yu, F. Fu, W. Han, G. Li, J. Xie, Y. Song, M.T. Swihart, E. Song, Dual recognition strategy for specific and sensitive detection of bacteria using aptamer-coated magnetic beads and antibiotic-capped gold nanoclusters, Analytical chemistry 88 (2016) 820–825.
[30] R.T. Hayden, L.K. Clinton, C. Hewitt, T. Koyamatsu, Y. Sun, G. Jamison, R. Perkins, L. Tang, S. Pounds, M.J. Bankowski, Rapid antimicrobial susceptibility testing using forward laser light scatter technology, Journal of clinical microbiology 54 (2016) 2701–2706.
[31] U. Sharaha, E. Rodriguez-Diaz, K. Riesenberg, I.J. Bigio, M. Huleihel, A. Salman, Using infrared spectroscopy and multivariate analysis to detect antibiotics' resistant Escherichia coli bacteria, Analytical chemistry 89 (2017) 8782–8790.
[32] L. Zeiri, B. Bronk, Y. Shabtai, J. Eichler, S. Efrima, Surface-enhanced Raman spectroscopy as a tool for probing specific biochemical components in bacteria, Applied Spectroscopy 58 (2004) 33–40.
[33] S. Pahlow, S. Meisel, D. Cialla-May, K. Weber, P. Rösch, J. Popp, Isolation and identification of bacteria by means of Raman spectroscopy, Advanced drug delivery reviews 89 (2015) 105–120.
[34] S. Holler, R.K. Chang, S.C. Hill, R.G. Pinnick, S. Niles, J.R. Bottiger, Single-shot fluorescence spectra of individual micrometer-sized bioaerosols illuminated by a 351-or a 266-nm ultraviolet laser, Optics letters 24 (1999) 116–118.
[35] P.M. Pellegrino, N.F. Fell Jr, J.B. Gillespie, Enhanced spore detection using dipicolinate extraction techniques, Analytica Chimica Acta 455 (2002) 167–177.
[36] J. Kusters, W.B. van Leeuwen, K. Maquelin, H. Blok, H. Willemse, L. de Graaf-Miltenburg, A. Fluit, A. Troelstra, Raman spectroscopy-based identification of nosocomial outbreaks of the clonal bacterium Escherichia coli, European Journal of Clinical Microbiology & Infectious Diseases 35 (2016) 83–87.
[37] Y. Cheong, Y. Jin Kim, H. Kang, S. Choi, H. Joo Lee, L abel-free identification of antibiotic resistant isolates of living E scherichia coli: P ilot study, Microscopy research and technique 80 (2017) 177–182.
[38] K. Hamasha, Q.I. Mohaidat, R.A. Putnam, R.C. Woodman, S. Palchaudhuri, S.J. Rehse, Sensitive and specific discrimination of pathogenic and nonpathogenic Escherichia coli using Raman spectroscopy—a comparison of two multivariate analysis techniques, Biomedical optics express 4 (2013) 481–489.
[39] M. Kahraman, M.M. Yazici, F. Şahin, Ö.F. Bayrak, M. Çulha, Reproducible surface-enhanced Raman scattering spectra of bacteria on aggregated silver nanoparticles, Applied spectroscopy 61 (2007) 479–485.
[40] M. Kahraman, M.M. Yazıcı, F. Şahin, M. Culha, Convective assembly of bacteria for surface-enhanced Raman scattering, Langmuir 24 (2008) 894–901.
[41] Y. Cheong, Y.J. Kim, H. Kang, S. Choi, H.J. Lee, Rapid label-free identification of Klebsiella pneumoniae antibiotic resistant strains by the drop-coating deposition surface-enhanced Raman scattering method, Spectrochimica Acta Part A: Molecular and Biomolecular Spectroscopy 183 (2017) 53–59.
[42] J. Li, C. Wang, H. Kang, L. Shao, L. Hu, R. Xiao, S. Wang, B. Gu, Label-free identification carbapenem-resistant Escherichia coli based on surface-enhanced resonance Raman scattering, RSC advances 8 (2018) 4761–4765.
[43] F.U. Ciloglu, A.M. Saridag, I.H. Kilic, M. Tokmakci, M. Kahraman, O. Aydin, Identification of methicillin-resistant Staphylococcus aureus bacteria using surface-enhanced Raman spectroscopy and machine learning techniques, Analyst 145 (2020) 7559–7570.
[44] Y. Li, Z. Shen, S. Ding, S. Wang, A TaqMan-based multiplex real-time PCR assay for the rapid detection of tigecycline resistance genes from bacteria, faeces and environmental samples, BMC microbiology 20 (2020) 1–7.
[45] Z.-H. Cui, Z.-J. Zheng, T. Tang, Z.-X. Zhong, C.-Y. Cui, X.-L. Lian, L.-X. Fang, Q. He, X.-R. Wang, C. Chen, Rapid Detection of High-Level Tigecycline Resistance in Tet (X)-Producing Escherichia coli and Acinetobacter spp. Based on MALDI-TOF MS, Frontiers in Cellular and Infection, Microbiology 10 (2020).
[46] Z.-H. Cui, W.-N. Ni, T. Tang, B. He, Z.-X. Zhong, L.-X. Fang, L. Chen, C. Chen, C.-Y. Cui, Y.-H. Liu, Rapid detection of plasmid-mediated high-level tigecycline resistance in Escherichia coli and Acinetobacter spp, Journal of Antimicrobial Chemotherapy 75 (2020) 1479–1483.
[47] S. Nasir, M.I. Majeed, H. Nawaz, N. Rashid, S. Ali, S. Farooq, M. Kashif, S. Rafiq, S. Bano, M.N. Ashraf, Surface enhanced Raman spectroscopy of RNA samples extracted from blood of hepatitis C patients for quantification of viral loads, Photodiagnosis and Photodynamic Therapy 33 (2020) 102152.
[48] J. Bajwa, H. Nawaz, M.I. Majeed, A.I. Hussain, S. Farooq, N. Rashid, M.A. Bakkar, S. Ahmad, H. Hyat, S. Bashir, Quantitative analysis of solid dosage forms of

cefixime using Raman spectroscopy, Spectrochimica Acta Part A: Molecular and Biomolecular Spectroscopy 238 (2020) 118446.
[49] M.A. Bakkar, H. Nawaz, M.I. Majeed, A. Naseem, A. Ditta, N. Rashid, S. Ali, J. Bajwa, S. Bashir, S. Ahmad, Raman spectroscopy for the qualitative and quantitative analysis of solid dosage forms of Sitagliptin, Spectrochimica Acta Part A: Molecular and Biomolecular Spectroscopy 245 (2021) 118900.
[50] E. Wiercigroch, E. Szafraniec, K. Czamara, M.Z. Pacia, K. Majzner, K. Kochan, A. Kaczor, M. Baranska, K. Malek, Raman and infrared spectroscopy of carbohydrates: A review, Spectrochimica Acta Part A: Molecular and Biomolecular Spectroscopy 185 (2017) 317–335.
[51] K.C. Schuster, I. Reese, E. Urlaub, J.R. Gapes, B. Lendl, Multidimensional information on the chemical composition of single bacterial cells by confocal Raman microspectroscopy, Analytical chemistry 72 (2000) 5529–5534.
[52] R.M. Jarvis, R. Goodacre, Discrimination of bacteria using surface-enhanced Raman spectroscopy, Analytical Chemistry 76 (2004) 40–47.
[53] Y. Liu, H. Zhou, Z. Hu, G. Yu, D. Yang, J. Zhao, Label and label-free based surface-enhanced Raman scattering for pathogen bacteria detection: A review, Biosensors and Bioelectronics 94 (2017) 131–140.
[54] A. Walter, A. März, W. Schumacher, P. Rösch, J. Popp, Towards a fast, high specific and reliable discrimination of bacteria on strain level by means of SERS in a microfluidic device, Lab on a Chip 11 (2011) 1013–1021.
[55] N.A. Mungroo, G. Oliveira, S. Neethirajan, SERS based point-of-care detection of food-borne pathogens, Microchimica acta 183 (2016) 697–707.
[56] M. Demirel, P. Kao, N. Malvadkar, H. Wang, X. Gong, M. Poss, D. Allara, Bio-organism sensing via surface enhanced Raman spectroscopy on controlled metal/polymer nanostructured substrates, Biointerphases 4 (2009) 35–41.
[57] Y. Liu, Y.-R. Chen, X. Nou, K. Chao, Potential of surface-enhanced Raman spectroscopy for the rapid identification of Escherichia coli and Listeria monocytogenes cultures on silver colloidal nanoparticles, Applied spectroscopy 61 (2007) 824–831.
[58] W. Wang, V. Hynninen, L. Qiu, A. Zhang, T. Lemma, N. Zhang, H. Ge, J.J. Toppari, V.P. Hytönen, J. Wang, Synergistic enhancement via plasmonic nanoplate-bacteria-nanorod supercrystals for highly efficient SERS sensing of food-borne bacteria, Sensors and Actuators B: Chemical 239 (2017) 515–525.
[59] P. Kao, N.A. Malvadkar, M. Cetinkaya, H. Wang, D.L. Allara, M.C. Demirel, Surface-enhanced Raman detection on metalized nanostructured poly (p-xylylene) films, Advanced Materials 20 (2008) 3562–3565.
[60] P. Filzmoser, K. Varmuza, M.P. Filzmoser, Introduction to Multivariate Statistical Analysis in Chemometrics (2009).
[61] C. Nieva, M. Marro, N. Santana-Codina, S. Rao, D. Petrov, A. Sierra, The lipid phenotype of breast cancer cells characterized by Raman microspectroscopy: towards a stratification of malignancy, PloS one 7 (2012) e46456.
[62] T. Dieing, O. Hollricher, J. Toporski, Confocal raman microscopy, Springer, 2011.
[63] S. Preciado-Flores, D.A. Wheeler, T.M. Tran, Z. Tanaka, C. Jiang, M. Barboza-Flores, F. Qian, Y. Li, B. Chen, J.Z. Zhang, SERS spectroscopy and SERS imaging of Shewanella oneidensis using silver nanoparticles and nanowires, Chemical Communications 47 (2011) 4129–4131.
[64] X. Chen, M. Tang, Y. Liu, J. Huang, Z. Liu, H. Tian, Y. Zheng, M.L. de la Chapelle, Y. Zhang, W. Fu, Surface-enhanced Raman scattering method for the identification of methicillin-resistant Staphylococcus aureus using positively charged silver nanoparticles, Microchimica Acta 186 (2019) 102.
[65] Y. Yan, Y. Nie, L. An, Y.-Q. Tang, Z. Xu, X.-L. Wu, Improvement of Surface-Enhanced Raman Scattering Method for Single Bacterial Cell Analysis, Frontiers in bioengineering and biotechnology 8 (2020) 1091.
[66] G. Naja, P. Bouvrette, S. Hrapovic, J.H. Luong, Raman-based detection of bacteria using silver nanoparticles conjugated with antibodies, Analyst 132 (2007) 679–686.
[67] D.D. Galvan, Q. Yu, Surface-Enhanced Raman Scattering for Rapid Detection and Characterization of Antibiotic-Resistant Bacteria, Advanced healthcare materials 7 (2018) 1701335.
[68] C. Fan, Z. Hu, A. Mustapha, M. Lin, Rapid detection of food- and waterborne bacteria using surface-enhanced Raman spectroscopy coupled with silver nanosubstrates, Applied Microbiology and Biotechnology 92 (2011) 1053–1061.
[69] D. Yang, H. Zhou, C. Haisch, R. Niessner, Y. Ying, E. Reproducible, coli detection based on label-free SERS and mapping, Talanta 146 (2016) 457–463.
[70] J.-S. Lee, A.K.R. Lytton-Jean, S.J. Hurst, C.A. Mirkin, Silver Nanoparticle−Oligonucleotide Conjugates Based on DNA with Triple Cyclic Disulfide Moieties, Nano Letters 7 (2007) 2112–2115.
[71] S. Pal, Y.K. Tak, J.M. Song, Does the antibacterial activity of silver nanoparticles depend on the shape of the nanoparticle?, A study of the gram-negative bacterium Escherichia coli, Applied and environmental microbiology 73 (2007) 1712–1720.
[72] J.S. Kim, E. Kuk, K.N. Yu, J.-H. Kim, S.J. Park, H.J. Lee, S.H. Kim, Y.K. Park, Y.H. Park, C.-Y. Hwang, Antimicrobial effects of silver nanoparticles, Nanomedicine: Nanotechnology, Biology and Medicine 3 (2007) 95–101.
[73] I. Sondi, B. Salopek-Sondi, Silver nanoparticles as antimicrobial agent: a case study on E. coli as a model for Gram-negative bacteria, Journal of colloid and interface science 275 (2004) 177–182.
[74] J.R. Morones, J.L. Elechiguerra, A. Camacho, K. Holt, J.B. Kouri, J.T. Ramírez, M.J. Yacaman, The bactericidal effect of silver nanoparticles, Nanotechnology 16 (2005) 2346.
[75] A.M.E. Badawy, T.P. Luxton, R.G. Silva, K.G. Scheckel, M.T. Suidan, T.M. Tolaymat, Impact of environmental conditions (pH, ionic strength, and electrolyte type) on the surface charge and aggregation of silver nanoparticles suspensions, Environmental science & technology 44 (2010) 1260–1266.
[76] E. Amato, Y.A. Diaz-Fernandez, A. Taglietti, P. Pallavicini, L. Pasotti, L. Cucca, C. Milanese, P. Grisoli, C. Dacarro, J.M. Fernandez-Hechavarria, Synthesis, characterization and antibacterial activity against Gram positive and Gram negative bacteria of biomimetically coated silver nanoparticles, Langmuir 27 (2011) 9165–9173.
[77] J.C. Park, G.E. Jeon, C.S. Kim, J.H. Seo, Effect of the size and shape of silver nanoparticles on bacterial growth and metabolism by monitoring optical density and fluorescence intensity, Biotechnology and Bioprocess Engineering 22 (2017) 210–217.
[78] L. Cui, S. Chen, K. Zhang, Effect of toxicity of Ag nanoparticles on SERS spectral variance of bacteria, Spectrochimica Acta Part A: Molecular and Biomolecular Spectroscopy 137 (2015) 1061–1066.
[79] S. Bashir, H. Nawaz, M.I. Majeed, M. Mohsin, S. Abdullah, S. Ali, N. Rashid, M. Kashif, F. Batool, M. Abubakar, S. Ahmad, A. Abdulraheem, Rapid and sensitive discrimination among carbapenem resistant and susceptible E. coli strains using Surface Enhanced Raman Spectroscopy combined with chemometric tools, Photodiagnosis and Photodynamic Therapy (2021) 102280.
[80] Y. Wang, K. Lee, J. Irudayaraj, Silver nanosphere SERS probes for sensitive identification of pathogens, The Journal of Physical Chemistry C 114 (2010) 16122–16128.
[81] K. Czamara, K. Majzner, M.Z. Pacia, K. Kochan, A. Kaczor, M. Baranska, Raman spectroscopy of lipids: a review, Journal of Raman Spectroscopy 46 (2015) 4–20.
[82] Y. Wang, S. Ravindranath, J. Irudayaraj, Separation and detection of multiple pathogens in a food matrix by magnetic SERS nanoprobes, Analytical and Bioanalytical Chemistry 399 (2011) 1271–1278.
[83] A. Barhoumi, D. Zhang, F. Tam, N.J. Halas, Surface-enhanced Raman spectroscopy of DNA, Journal of the American Chemical Society 130 (2008) 5523–5529.
[84] S. Efrima, L. Zeiri, Understanding SERS of bacteria, Journal of Raman Spectroscopy: An International Journal for Original Work in all Aspects of Raman Spectroscopy, Including Higher Order Processes, and also Brillouin and Rayleigh Scattering 40 (2009) 277–288.
[85] T.-T. Liu, Y.-H. Lin, C.-S. Hung, T.-J. Liu, Y. Chen, Y.-C. Huang, T.-H. Tsai, H.-H. Wang, D.-W. Wang, J.-K. Wang, A high speed detection platform based on surface-enhanced Raman scattering for monitoring antibiotic-induced chemical changes in bacteria cell wall, PloS one 4 (2009) e5470.
[86] W.R. Premasiri, J.C. Lee, A. Sauer-Budge, R. Theberge, C.E. Costello, L.D. Ziegler, The biochemical origins of the surface-enhanced Raman spectra of bacteria: a metabolomics profiling by SERS, Analytical and bioanalytical chemistry 408 (2016) 4631–4647.
[87] U. Rinas, K. Hellmuth, R. Kang, A. Seeger, H. Schlieker, Entry of Escherichia coli into stationary phase is indicated by endogenous and exogenous accumulation of nucleobases, Applied and Environmental Microbiology 61 (1995) 4147–4151.
[88] C.-Y. Liu, Y.-Y. Han, P.-H. Shih, W.-N. Lian, H.-H. Wang, C.-H. Lin, P.-R. Hsueh, J.-K. Wang, Y.-L. Wang, Rapid bacterial antibiotic susceptibility test based on simple surface-enhanced Raman spectroscopic biomarkers, Scientific reports 6 (2016) 1–15.
[89] H. Zhou, D. Yang, N.P. Ivleva, N.E. Mircescu, S.r. Schubert, R. Niessner, A. Wieser, C. Haisch, Label-free in situ discrimination of live and dead bacteria by surface-enhanced Raman scattering, Analytical chemistry, 87 (2015) 6553-6561.
[90] W. Yang, I.F. Moore, K.P. Koteva, D.C. Bareich, D.W. Hughes, G.D. Wright, TetX is a flavin-dependent monooxygenase conferring resistance to tetracycline antibiotics, Journal of Biological Chemistry 279 (2004) 52346–52352.